Anisotropic self-diffusion in ferrofluids studied via Brownian dynamics simulations

Patrick Ilg[1,2,*] and Martin Kröger[3]
[1]*Institut für Theoretische Physik, Technische Universität Berlin, Hardenbergstr. 36, D-10623 Berlin, Germany*
[2]*Département de Physique des Matériaux, Université Claude Bernard Lyon1, F-69622 Villeurbanne, France*
[3]*Polymer Physics, ETH Zürich, Wolfgang-Pauli-Str. 10, CH-8093 Zürich, Switzerland*
(Received 22 March 2005; published 13 September 2005)

The anisotropic self-diffusion in ferrofluids in the presence of a magnetic field is studied by Brownian dynamics simulations. It is found that the diffusion parallel to the magnetic field is hindered when compared to the case without field. Depending on the strength of dipolar interactions, the diffusion perpendicular to the applied field is either enhanced or hindered due to the field. The average diffusion coefficient is found to decrease with increasing concentration and dipolar interaction strength, but to be independent of the magnetic field strength for moderate dipolar interactions. Comparison to mean-field models show agreement for moderate dipolar interaction strengths but significant deviations in the regime of strong dipolar interactions.

DOI: 10.1103/PhysRevE.72.031504 PACS number(s): 83.10.Mj, 75.50.Mm, 66.10.Cb, 47.65.+a

I. INTRODUCTION

Colloidal suspensions of nanosized magnetic particles, so-called ferrofluids, have attracted considerable attention in recent years since their physical properties can be manipulated by an external magnetic field [1]. While anisotropic, field-dependent gradient diffusion in ferrofluids has been observed in recent experiments [2,3] and studied theoretically in [4–6], self- (or tracer) diffusion in ferrofluids has been less studied. Experimental and numerical results on self-diffusion in a quasi-two-dimensional ferrofluid are reported in [7]. A hydrodynamic theory of self-diffusion in ferrofluids is presented in [8,9]. However, the effect of a magnetic field on the self-diffusion coefficients has not been investigated in these works.

In the present study, we perform extensive Brownian dynamics (BD) simulations of a monodisperse model ferrofluid in order to study the effect of a magnetic field on the coefficients of self-diffusion. Different concentrations and dipolar interaction strengths are considered. The simulation results clearly show anisotropic self-diffusion in the presence of a magnetic field. The field dependence of the self-diffusion coefficients can be interpreted within a mean-field model. Similarities with gradient diffusion coefficients are discussed.

The paper is organized as follows: in Sec. II, the model system is introduced. In Sec. III, the predictions of simplified mean-field models are given. The simulation results are presented in Sec. IV, together with a comparison to the mean-field predictions. Finally, some conclusions are offered in Sec. V.

II. MODEL SYSTEM

Let us consider a system of N identical, spherical, Brownian particles of diameter d_c in a cubic simulation box of volume V. It is assumed, that the particles are ferromagnetic hard, monodomain particles with an embedded point dipole of strength m. The magnetic volume fraction occupied by the particles is $\phi=n\pi d_c^3/6$, where $n=N/V$ is the number density. If $\mathbf{r}_i$ and $\mathbf{u}_i$ denote the position and orientation of the magnetic dipole of particle i, respectively, the total interaction potential in the presence of a homogeneous internal magnetic field $\mathbf{H}$ is given by

$$\Phi^{\mathrm{tot}}=\frac{1}{2}\sum_{i\neq j}\{\Phi^{\mathrm{s}}(r_{ij})+\Phi^{\mathrm{dd}}(\mathbf{r}_{ij},\mathbf{u}_i,\mathbf{u}_j)\}-k_BTh\sum_i \mathbf{u}_i\cdot\hat{\mathbf{H}}, \tag{1}$$

where $\mathbf{r}_{ij}=\mathbf{r}_i-\mathbf{r}_j$, $r_{ij}=|\mathbf{r}_{ij}|$ is the distance between particles i and j, $\hat{\mathbf{H}}=\mathbf{H}/|\mathbf{H}|$ denotes the direction of the magnetic field and $h=\mu_0 m|\mathbf{H}|/(k_BT)$ is the Langevin parameter. The dipolar interaction potential is given by

$$\Phi^{\mathrm{dd}}(\mathbf{r},\mathbf{u},\mathbf{u}')=-3k_BT\lambda\left(\frac{d_c}{r}\right)^3\mathbf{u}\cdot\left(\hat{\mathbf{r}}\hat{\mathbf{r}}-\frac{1}{3}\mathbf{1}\right)\cdot\mathbf{u}', \tag{2}$$

where $r=|\mathbf{r}|$ is the distance between the particles, $\hat{\mathbf{r}}=\mathbf{r}/r$ denotes the unit vector and

$$\lambda=\frac{\mu_0 m^2}{4\pi k_BTd_c^3} \tag{3}$$

is the dimensionless dipolar interaction parameter. In order to prevent permanent agglomeration due to van der Waals forces, the ferromagnetic particles are covered with a polymeric shell [10]. According to Rosensweig [10], the resulting steric repulsion between two particles can approximately be described by the repulsive potential

$$\Phi^{\mathrm{s}}(r)=N_{\mathrm{p}}k_BT\left[1+\frac{1}{t}-\frac{r}{2\delta}\left\{\ln\left(\frac{1+t}{r/d_c}\right)+1\right\}\right] \tag{4}$$

for $d_c\leqslant r\leqslant d_c+2\delta$ and $\Phi^{\mathrm{s}}(r)=0$ else. Here, δ denotes the length and N_{p} the number of adsorbed polymeric molecules on the surface of a particle and $t=2\delta/d_c$. It is assumed that the polymeric shell prevents permanent agglomeration of the particles. Thus, N_{p} is chosen large enough so that van der

*Corresponding author. Electronic address: ilg@physik.tu-berlin.de

Waals interactions can be neglected. As was done in a previous work [11], we assume that the system is surrounded by a homogeneous medium with infinite magnetic permeability. These metallic boundary conditions ensure that the applied external field is identical to the internal field $\mathbf{H}$.

A. Equations of motion

Friction forces due to the solvent lead to an overdamped translational and orientational motion of the ferromagnetic particles. The resulting Brownian dynamics is described by the Langevin type equations of motion [12]

$$d\mathbf{r}_i = \frac{1}{\xi}\mathbf{F}_i dt + \sqrt{\frac{2k_BT}{\xi}}d\mathbf{W}_i, \tag{5}$$

where $\mathbf{F}_i = -\partial\Phi^{\mathrm{tot}}/\partial\mathbf{r}_i$ is the total force acting on particle i with Φ^{tot} from Eq. (1). Similarly, for the orientational motion

$$d\mathbf{u}_i = \left[\frac{1}{\xi_{\mathrm{r}}}\mathbf{N}_i dt + \sqrt{\frac{2k_BT}{\xi_{\mathrm{r}}}}d\mathbf{W}_i\right] \times \mathbf{u}_i, \tag{6}$$

where $\mathbf{N}_i = -\mathcal{L}_i\Phi^{\mathrm{tot}}$, $\mathcal{L}_i = \mathbf{u}_i \times \partial/\partial\mathbf{u}_i$, is the total torque on particle i due to dipolar interactions and the external field $\mathbf{H}$. In Eqs. (5) and (6), the translational and rotational friction coefficients ξ and ξ_{r} have been introduced. For hard spheres of diameter d in a solvent with viscosity η, these friction coefficients are given by $\xi = 3\pi\eta d$ and $\xi_{\mathrm{r}} = \pi\eta d^3$. For a general, continuous interaction potential $\Phi_{\mathrm{s}}(r)$, an equivalent hard sphere diameter d is defined by $d_{\mathrm{HS}} = \int_0^\infty dr\{1 - \exp[-\beta\Phi_{\mathrm{s}}(r)]\}$ based on the virial equation of state [13].

The random forces due to the solvent are modeled with the help of independent Wiener processes $\mathbf{W}$ (Gaussian random variables) with zero mean $\langle \mathbf{W}_i(t)\rangle = 0$ and variance $\langle \mathbf{W}_i(t)\mathbf{W}_j(t')\rangle = \mathbf{1}\delta_{ij}\min(t,t')$ [12]. Thus, the present model corresponds to the so-called free-draining limit, where hydrodynamic interactions between the particles are neglected. In general, the contribution of hydrodynamic interactions to diffusion coefficients is significant (see [7] for the influence of hydrodynamic interactions in quasi-two-dimensional ferrofluids). One might speculate that their influence on the anisotropy of the diffusion might be much weaker. In any case, we believe that it is helpful to separate different contributions and study here the dynamics of the interacting many-particle system in the absence of hydrodynamic interactions. In a similar spirit, the theoretical approach proposed in [8,9] neglects hydrodynamic interactions.

B. Self-diffusion coefficients

Coefficients of self-diffusion (sometimes also called tracer diffusion) are defined with the help of the mean-square displacement of a tagged particle in a sea of like particles by

$$\lim_{t\to\infty}\langle \Delta r_\alpha(t)\Delta r_\beta(t)\rangle = 2D_{\alpha\beta}\, t, \tag{7}$$

with $\Delta r_\alpha(t) \equiv r_\alpha(t) - r_\alpha(0)$ the Cartesian component of the displacement at time t [14]. The coefficients $D_{\alpha\beta}$, $\alpha \in \{x,y,z\}$, quantify diffusion parallel to the x, y, and z axes. The average is performed over the ensemble of realizations. The coefficients $D_{\alpha\beta}$ can be evaluated with the solution trajectories of Eqs. (5) and (6). In the absence of particle interactions, Eq. (5) is solved by $\mathbf{r}_j(t) = \mathbf{r}_j(0) + \sqrt{2k_BT/\xi}\mathbf{W}_j(t)$. With the properties of the above Wiener process, Eq. (7) basically holds with the single particle diffusion coefficient $D = D_{\mathrm{sp}} \equiv k_BT/\xi$, and $\forall_\alpha D_{\alpha\alpha} = D$ for Eq. (7). Interactions between the particles are expected to change the value for D. In particular, due to the translational-rotational coupling, the self-diffusion becomes anisotropic in the presence of a magnetic field, i.e., $D_{\alpha\alpha} \neq D$ and $D \neq D_{\mathrm{sp}}$, if both mechanisms are active.

If the magnetic field is oriented in the z direction, the diffusion coefficients parallel and perpendicular to the applied field are defined by

$$D_\parallel = D_{zz}, \quad D_\perp = \frac{1}{2}(D_{xx} + D_{yy}). \tag{8}$$

The average self-diffusion coefficient is given by $\bar{D} = (D_\parallel + 2D_\perp)/3$. The above model leads to diffusion coefficients which depend, in particular, independently on concentration ϕ, Langevin parameter h, and the interaction strength λ.

Unfortunately, the Langevin Eqs. (5) and (6) cannot be solved in the closed form in general. These equations can be integrated numerically, however, via Brownian dynamics which permits to evaluate Eq. (7), as will be described in Sec. II D. In order to improve the statistics, it is common to average Eq. (7) over all particles. Further, we consider in Sec. III a simplified, mean-field model, that allows us to calculate the effective diffusion coefficients analytically.

C. Coefficients of gradient diffusion

The self-diffusion coefficients $D_{\alpha\beta}$ defined in Eq. (7) describing the dynamics of tagged particles must not be confused with the gradient (or chemical) diffusion coefficient $D^{\boldsymbol{\nabla}}_{\alpha\beta}$. The latter is defined by

$$j_\alpha = -D^{\boldsymbol{\nabla}}_{\alpha\beta}\boldsymbol{\nabla}_\beta\rho, \tag{9}$$

where j_α are the Cartesian components of the diffusion current and ρ the mass density [14,15].

A simple relation between the self-diffusion and gradient-diffusion coefficients exists in nonmagnetic fluids if the cross correlations between the velocity of different particles are negligible [14]. In that case, it can be shown that the diffusion coefficients are related by the so-called Darken equation $D^{\boldsymbol{\nabla}} = KD$, with the dimensionless coefficient $K = nk_BT/\tilde{\chi}_{\mathrm{T}}$, $n = N/V$, and $\tilde{\chi}_{\mathrm{T}}$ is the isothermal compressibility [14]. The quantity $D^{\boldsymbol{\nabla}}/K$ is sometimes called "corrected" gradient-diffusion coefficient. For some systems, the validity of the Darken equation could be established (e.g., see [15–17]). From the Darken equation it is obvious that D and $D^{\boldsymbol{\nabla}}$ show different dependencies on the concentration since the coefficient K is concentration dependent. In magnetic fluids, the applicability of the Darken equation is even more questionable. In this case, local concentration gradients lead to gradients in the local magnetic field that give rise to ponderomotive forces that influence the diffusion properties.

In principle, gradient-diffusion coefficients $D^{\boldsymbol{\nabla}}$ may be extracted from the mean-square displacement of the center of

mass position [14], in analogy to Eq. (7). For the special case of Brownian dynamics without hydrodynamic interactions, however, the thus-defined gradient-diffusion coefficient reduces to the single particle diffusion coefficient since the interparticle interactions preserve the center of mass momentum. Therefore, we focus on the self-diffusion coefficient in the present study, but will also mention hints toward relationships between these coefficients in Sec. III. Further, methods for calculating the collective diffusivity (and, therefore, also the gradient diffusivity from its short wavelength limit) from suspension microstructure relaxation measurements during Stokesian dynamics [18], and the intermediate scattering function evaluations during accelerated Stokesian dynamics [15] simulations have been reported, and applied to noncolloidal hard sphere suspensions.

D. Numerical implementation

As reference length and time scales, we choose the particle core diameter d_c and the time to diffuse the core diameter $\tau_0 = d_c^2 \xi/(6k_BT)$. Defining dimensionless position vectors $\mathbf{r}_j^* = \mathbf{r}_j/d_c$ and time $t^* = t/\tau_0$, the equations of motion (5) and (6) can be written in dimensionless form,

$$d\mathbf{r}_i^* = (1/\xi^*)\mathbf{F}_i^* dt^* + \sqrt{2/\xi^*}\, d\mathbf{W}_i^*, \tag{10}$$

$$d\mathbf{u}_i = [(1/\xi_r^*)\mathbf{N}_i^* dt^* + \sqrt{2/\xi_r^*}\, d\mathbf{W}_i^*] \times \mathbf{u}_i. \tag{11}$$

The dimensionless friction coefficients are defined by $\xi^* = d_c^2 \xi/(k_BT\tau_0)$ and $\xi_r^* = \xi_r/(k_BT\tau_0)$. In Eqs. (10) and (11), the dimensionless force $\mathbf{F}_i^* = (d_c/k_BT)\mathbf{F}_i$ and torque $\mathbf{N}_i^* = \mathbf{N}_i/(k_BT)$ have been used as well as the dimensionless Wiener increment $d\mathbf{W}^* = d\mathbf{W}/\sqrt{\tau_0}$. For the parameters investigated here, the shell thickness δ of the polymeric layer is small enough such that the diameter d entering the single particle friction coefficients is well approximated by d_c. For the chosen time scale τ_0 we, therefore, have $\xi^* = 6$ and $\xi_r^* = \xi^*/3$. The dimensionless control parameters entering the model are the volume fraction ϕ, Langevin parameter h, dipolar interaction strength λ, the strength of the steric repulsion N_p, and the ratio of the thickness of polymeric shell over the core diameter $t = 2\delta/d_c$. In order to minimize surface effects, periodic boundary conditions are applied. The long range nature of the dipolar interactions is accounted for by the reaction field method [19]. In this method, the dipolar interactions for a pair of particles closer than a cutoff radius r_{cut} are calculated explicitly, while the effect of more remote particles is estimated by continuum arguments [19].

Equations (10) and (11) are integrated numerically with a second order scheme preserving exactly the normalization of the unit vectors $\mathbf{u}_j$. A weak first order scheme due to Ermak [12,20] was used in order to integrate Eq. (10) numerically. Several checks with a second order predictor-corrector scheme (also termed stochastic Runge-Kutta method [20]) have been performed, leading to very similar results.

The time step of the numerical integration was chosen as $\Delta t = 5 \times 10^{-4}\tau_0$. Systems of $N = 10\,976$ particles are considered with different dipolar interaction strengths $\lambda = 0.25, \ldots, 8$ and volume fractions of $\phi = 0.01, \ldots, 0.20$. The strength of the repulsive potential (4) was chosen as $N_p = 100$ and $N_p = 314$. Since nearly identical results are obtained for both values, we chose to present the results for $N_p = 100$ only. A fixed ratio $t = 0.25$ of twice the length of the adsorbed molecules over the diameter of the magnetic core was chosen. The cutoff radius was chosen as $r_{cut} = 3d_c$ for $\lambda \leqslant 4$ and $r_{cut} = 5d_c$ for $\lambda > 4$. Some simulations with a larger values of r_{cut} have been performed, showing very similar results.

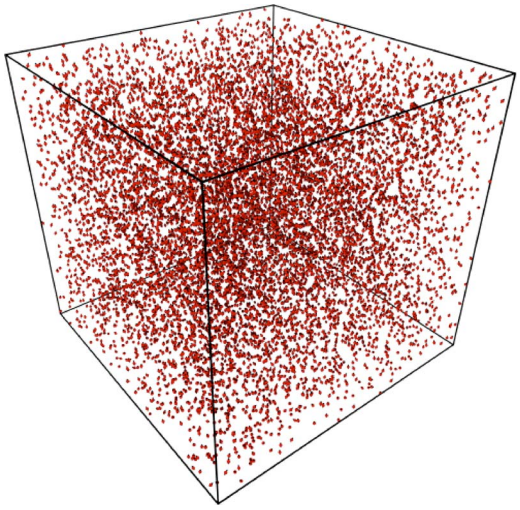

FIG. 1. (Color online) Snapshots of the configurations after equilibration. The volume fraction was chosen as $\phi = 0.02$, dipolar interaction parameter $\lambda = 1$. A magnetic field was applied in the vertical direction. The dimensionless strength of the magnetic field was chosen $h = 10$.

Starting from initial configurations with the particles on regular lattice sites and random dipole orientations, the system is evolved for 4×10^4 time steps in order to ensure that the equilibrium state has been reached. A snapshot of a configuration is shown in Fig. 1. The mean-square displacement of the particles is extracted for another 2.6×10^5 time steps. The diffusion coefficients are extracted from linear fits to the mean-square displacement according to Eq. (7). In order to provide better statistics, the evaluation of the mean-square displacement is periodically repeated in intervals of $T = 40\tau_0$. Figure 2 shows the resulting mean-square displacement for $\phi = 0.05$, $\lambda = 4$, and $h = 20$. Several tests have been performed where the mean-square displacement was accumulated for the total simulation time. Negligible differences within the numerical uncertainties for the resulting diffusion coefficients are found, indicating that the long time limit has indeed been reached.

III. SIMPLIFIED MEAN-FIELD MODELS

In order to find a common description of rheological and dynamical properties, the application of the chain model [21] to the anisotropic diffusion in ferrofluids has been proposed in [6]. In the chain model [21], dipolar interactions between the ferromagnetic particles are approximately taken into account by considering a dilute solution of effective, ellipsoidal particles that result from temporary or permanent agglomera-

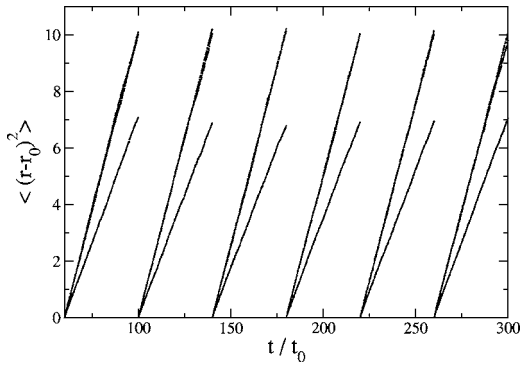

FIG. 2. The Cartesian components of the mean-square displacement $\langle(\Delta r_\alpha)^2\rangle/d_c^2$ as a function of reduced time. The upper two sets of data correspond to perpendicular displacements, while the lower one corresponds to parallel displacements with respect to the magnetic field. The volume fraction $\phi=0.05$, dipolar interaction parameter $\lambda=4$, and Langevin parameter $h=20$ have been chosen.

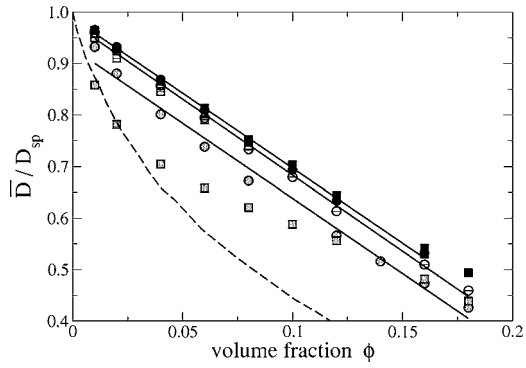

FIG. 3. The normalized average diffusion coefficient $\bar{D}/D_{sp}$ as a function of the volume fraction ϕ. Circles and squares correspond to Langevin parameters of $h=0$ and $h=20$, respectively. Solid, open, and shaded symbols correspond to $\lambda=1.0$, 2.0, and 4.0, respectively. The dashed line is the prediction of Ref. [8] for dipolar hard spheres.

tion. The axis ratio Q of the ellipsoid is related to the dipolar interaction strength λ. In the noninteracting case $\lambda\to 0$, one recovers the original, spherical particles with $Q=1$. The chain model has been applied successfully in order to describe viscous properties of nondilute ferrofluids [22]. Cluster formation in general leads to a distribution of cluster sizes [21]. Here, we restrict ourselves to interaction strengths that are weak enough so that the size distribution is rather narrow. In this case, the average over the size distribution can be approximated by the value for the average cluster size. Let $D_\parallel^0, D_\perp^0$ denote the self-diffusion coefficients parallel and perpendicular to the axes of the cluster, respectively. For prolate ellipsoidal particles one has $D_\parallel^0 > D_\perp^0$, while the opposite sign holds for oblate ellipsoidal particles. In [6] it is shown, under the assumption of magnetic field-independent coefficients $D_\parallel^0$ and $D_\perp^0$, that the effective diffusion coefficients parallel and perpendicular to the field are given by

$$D_\parallel(h) = \bar{D} + \frac{2}{3} c D_{sp} L_2(h), \tag{12}$$

$$D_\perp(h) = \bar{D} - \frac{1}{3} c D_{sp} L_2(h). \tag{13}$$

In Eqs. (12) and (13), the relative difference $c=(D_\parallel^0 - D_\perp^0)/D_{sp}$, the Langevin function $L_1(h)\equiv\coth(h)-1/h$, and $L_2(h)=1-3L_1(h)/h$ have been introduced. Within this model, the average diffusion coefficient is given by the value for the cluster

$$\bar{D} = \frac{D_\parallel^0 + 2D_\perp^0}{3}. \tag{14}$$

Both functions $L_1(h)$ and $L_2(h)$ monotonically increase with h, vanish at $h=0$, and asymptotically reach unity for large h. Equations (12)–(14) have been derived originally for the (corrected) gradient-diffusion coefficient. Since in the mean-field model [6], the velocities of different particles are assumed to be uncorrelated, the Darken equation holds and Eqs. (12)–(14) apply also for the self-diffusion coefficient. This result can also be obtained directly by calculating the mean-square displacement from the Fokker-Planck equation. Note, however, that in the case of gradient diffusion, extra contributions to the diffusion coefficients appear due to the spatially inhomogeneous local magnetic field and concentration. Within the mean-field model [6], these contributions modify the coefficient c in Eqs. (12) and (13) which then depends explicitly on the magnetic field, concentration, and dipolar interaction strength.

It is interesting to note that Eqs. (12) and (13) are very similar to the corresponding results obtained by Morozov [4] for the parallel and perpendicular gradient-diffusion coefficients. In [6] as well as in [4], the average diffusion coefficient $\bar{D}$ is predicted to be independent of the magnetic field strength, but still depends on λ and ϕ. Within the mean-field model [6], any concentration dependence enters through the shape of the cluster, more specifically, the "body-fixed" diffusion coefficients $D_\parallel^0$ and $D_\perp^0$. A nonzero magnetic field comes together with anisotropic diffusion, quantified through the difference between $D_\parallel(h)$ and $D_\perp(h)$ which, by construction, must vanish in the absence of symmetry imposed by the external field. The model, Eqs. (12)–(14), allows us to discuss the effect of the shape of clusters on the sign of $D_\parallel(h) - D_\perp(h)$.

IV. SIMULATION RESULTS

With the expectations of the foregoing section at hand, let us proceed with presenting simulation results of the model described in Sec. II. The results are obtained via Brownian dynamics simulation as was already described in Sec. II D.

Figure 3 shows the average self-diffusion coefficient $\bar{D}$, obtained via Eq. (7) as a function of the volume fraction ϕ. Without an applied magnetic field, $\bar{D}$ decreases linearly with ϕ within the range of parameters investigated here. A linear decrease of the average gradient diffusion coefficient with ϕ was predicted by Morozov [4]. For weak dipolar interactions $\lambda\lesssim 2$, the average diffusion coefficient $\bar{D}$ for $h=0$ and h

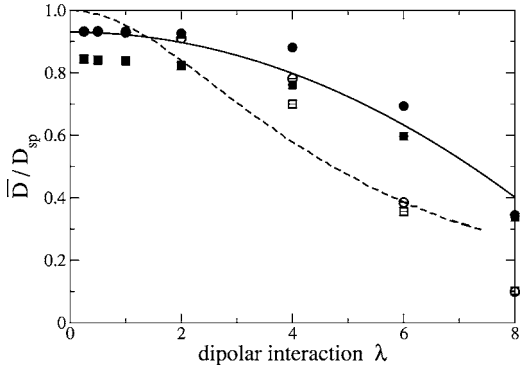

FIG. 4. The normalized average diffusion coefficient $\bar{D}/D_{sp}$ as a function of the dipolar interaction strength λ defined in Eq. (3). Circles and squares correspond to $\phi=0.02$ and $\phi=0.05$, solid and open symbols to Langevin parameters of $h=0$ and $h=20$, respectively. The dashed line is the prediction of Ref. [8] for dipolar hard spheres.

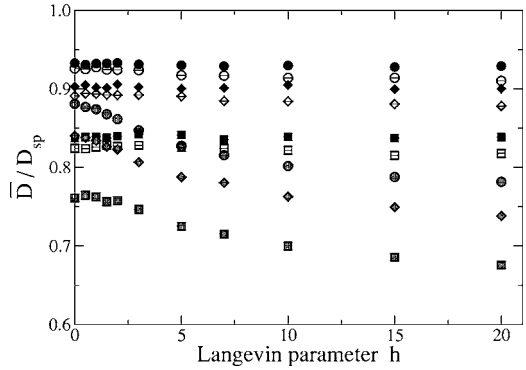

FIG. 5. The normalized average diffusion coefficient $\bar{D}/D_{sp}=(D_{\|}+2D_{\perp})/3D_{sp}$ is shown as a function of the Langevin parameter h. Circles, diamonds, and squares correspond to volume fractions of $\phi=0.02$, 0.03, and 0.05, respectively. Solid, open, and shaded symbols correspond to $\lambda=1.0$, 2.0, and 4.0, respectively.

$=20$ is found to be almost identical. For stronger dipolar interactions, $\lambda=4$, $\bar{D}$ decreases in the presence of a strong magnetic field for small enough concentrations. For $\phi\gtrsim 0.1$, within the error bars of the simulation, the same value for $\bar{D}$ is found for $h=0$ and $h=20$. This result indicates that the overall diffusion is hindered due to steric interactions between the particles. Dipolar interactions modify the average diffusion coefficient significantly only if the interaction strength is large enough. For further comparison, we included in Fig. 3 also the prediction of the hydrodynamic theory proposed in [8] for the case without the magnetic field. The data are taken from Ref. [8]. Note, however, that dipolar hard spheres were studied in [8] instead of the soft repulsion (4) used here. Due to the steric interactions (4), the minimal distance of two particles is greater than the core diameter d_c. The equivalent hard core diameter d_{HS}, introduced in Sec. II is $d_{HS}\approx 1.2d_c$ for the present choice of parameters. Therefore, the effective dipolar interaction parameter λ^*, the dimensionless dipolar interaction energy of two particles at contact, is reduced by a factor of $(d_c/d_{HS})^3 \approx 0.58$. Thus, the results of [8] for $\lambda^*=1.0$ correspond roughly to $\lambda\approx 1.7$. Although a slightly different system is studied in the present study, Fig. 3 seems to suggest that the diffusion is underpredicted in [8] in particular for higher volume fractions. The discrepancy becomes even larger if the corresponding hydrodynamic volume fraction is considered.

Figure 4 shows the average diffusion coefficient as a function of the dipolar interaction strength λ. In the absence of a magnetic field, $\bar{D}$ decreases only slightly with increasing λ for $\lambda\leqslant 4$, followed by a stronger decrease for $\lambda>4$. The presence of a strong magnetic field does not alter $\bar{D}$ for weak dipolar interactions, but leads to an even stronger decrease for $\lambda>4$. A quadratic fit to the data, motivated by the prediction [4] for the gradient-diffusion coefficient, is shown by the solid line in Fig. 4. The agreement with the numerical data, however, is not as good as in Fig. 3. Also shown in Fig. 4 is the prediction of [8] for $\phi=0.01$ for vanishing magnetic field. The dipolar interaction of parameter [8] has been multiplied by a factor $(d_{HS}/d_c)^3\approx 1.7$ in order to account for the different short range potentials. Figure 4 indicates that the dependence of the average diffusion coefficient on the dipolar interaction parameter is weaker than predicted in [8]. The difference becomes even more significant if higher volume fractions are considered.

The average diffusion coefficient $\bar{D}$ is shown in Fig. 5 as a function of the Langevin parameter h. For moderate dipolar interaction strengths $\lambda\lesssim 2$, $\bar{D}$ is found to be independent of h. This result is in agreement with the predictions of the mean-field model presented in Sec. III. For the strongest dipolar interaction studied, $\lambda=4$, the average diffusion coefficient $\bar{D}$ decreases with increasing h. This behavior is not captured by the mean-field model.

The anisotropy ratio of the diffusion coefficients $R\equiv(D_{\|}-D_{\perp})/(D_{\|}+2D_{\perp})$ is shown in Fig. 6 as a function of the Langevin parameter h. For moderate dipolar interaction strengths, $\lambda\lesssim 2$, the simulation results are well described by the relation $R\propto L_2(h)$ in accordance with the mean-field predictions (12) and (13). For stronger dipolar interactions, $\lambda=4$, deviations from this behavior occur. It is interesting to note that the simulation results show that $D_{\|}<D_{\perp}$, i.e., the diffusion perpendicular to the applied field is faster than in

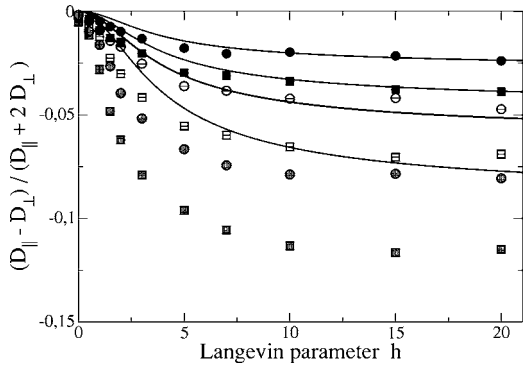

FIG. 6. The anisotropy ratio $R=(D_{\|}-D_{\perp})/(D_{\|}+2D_{\perp})$ of the diffusion coefficients as a function of the Langevin parameter h. The same symbols as in Fig. 5 are used. Solid lines are the predictions of the mean-field model, Eqs. (12) and (13).

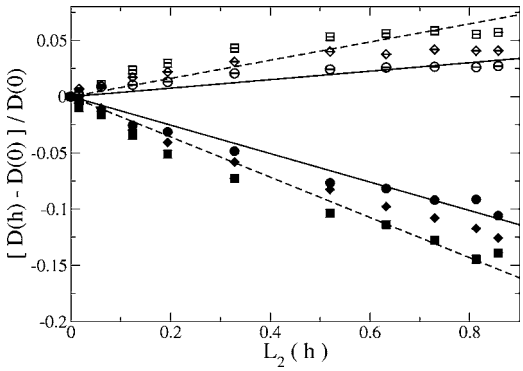

FIG. 7. The normalized diffusion coefficients $[D_{\parallel,\perp}(h) - D(0)]/D(0)$ as a function of the orientational order parameter L_2 defined in the text. The dipolar interaction parameter was chosen as $\lambda=2$. Circles, diamonds, and squares correspond to volume fractions of $\phi=0.02$, 0.03, and 0.05, respectively. Full symbols correspond to parallel diffusion coefficients; open symbols to perpendicular diffusion coefficients. Solid and dashed lines are the result of a linear fit.

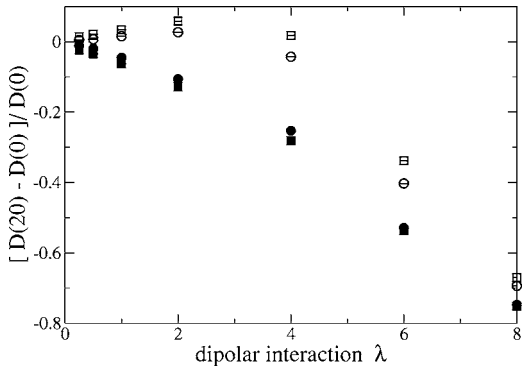

FIG. 8. The normalized diffusion coefficients $[D_{\parallel,\perp}(h) - D(0)]/D(0)$ for $h=20$ as a function of the dipolar interaction parameter λ defined in Eq. (3). Circles and squares correspond to volume fractions of $\phi=0.02$ and 0.05, respectively. Full symbols correspond to parallel diffusion coefficients; open symbols to perpendicular diffusion coefficients.

the parallel direction. This phenomenon is characteristic for oblate particles, where the axis ratio $Q<1$ [23]. Within the dynamical mean-field model [24], it is shown that the effect of weak dipolar interactions in moderately concentrated ferrofluids on dynamical properties like the nonequilibrium magnetization and viscosity can approximately be described by effective oblate ferromagnetic particles. Thus, the present simulation results are consistent with these findings and the corresponding simulation results for magnetic and viscous properties [11].

Figure 7 shows the relative change of the diffusion coefficients $[D_{\parallel,\perp}(h)-D(0)]/D(0)$ as a function of $L_2(h)$. As is demonstrated in Fig. 7, the simulation results are nicely described by a linear relation $D_{\parallel,\perp} \propto L_2$ as predicted by the mean-field model. The agreement is better for small concentrations where dipolar interactions and, therefore, cluster formation is weak. Note, however, that the slopes of the curves differ by more than a factor of two. Therefore, this feature is not captured correctly by the mean-field model (12) and (13).

Finally, Fig. 8 shows the dependence of the relative change of the diffusion coefficients $[D_{\parallel,\perp}(h)-D(0)]/D(0)$ on the dipolar interaction strength λ. A strong magnetic field of $h=20$ is applied. The volume fraction is chosen as $\phi=0.02$ and $\phi=0.05$. From Fig. 8 we observe that $D_{\parallel}(h)/D(0)$ is monotonically decreasing with increasing λ. The perpendicular diffusion coefficient is slightly increasing for $\lambda \leqslant 4$ and decreases for larger values of λ.

In order to better interpret the present results, the microstructure of the fluid is investigated by performing a cluster analysis. Similar to previous studies [25], agglomerates are defined by an energy criterion. In particular, we follow Ref. [25] and consider two particles to be bound if their dipolar interaction energy is less than $V_{\text{bond}}=-1.5\lambda^* k_B T$. This corresponds to 75% of the contact energy of two coaligned dipoles. The average cluster size is defined by

$$S_{\text{av}} = \left\langle \frac{\sum_s s n_s}{\sum_s n_s} \right\rangle, \tag{15}$$

where n_s is the number of clusters of size s. Figure 9 shows S_{av} as a function of the Langevin parameter h. From Fig. 9 we observe that for $\lambda \leqslant 4$, very few cluster formations occur and the magnetic field shows very little effect on S_{av}. For $\lambda=8$, cluster formation is more pronounced, with S_{av} increasing with increasing h. However, even for this value, S_{av} does not exceed 1.5 for the present choice of parameters. This result is not in contradiction to [25] where significant cluster formation was observed for $\lambda=8$ since a different repulsive potential was used in the latter study. Indeed, the effective dipolar interaction parameter λ^* corresponding to $\lambda=8$ is $\lambda^* \approx 7.9$ for the potential used in [25], but only $\lambda^* \approx 4.6$ for the present study.

V. CONCLUSIONS

Systematic Brownian dynamics simulations of a model ferrofluid in the presence of an applied magnetic field have

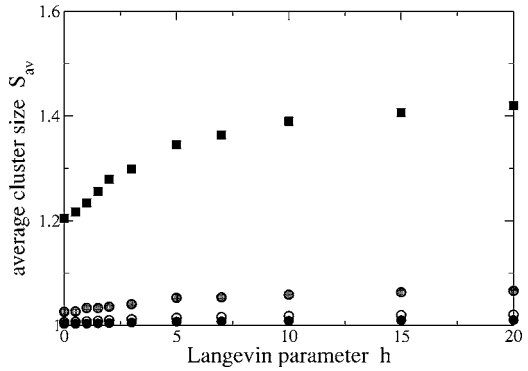

FIG. 9. The average cluster size S_{av}, defined in Eq. (15), as a function of the Langevin parameter h for $\phi=0.05$. Solid, open, and shaded circles correspond to $\lambda=1$, 2, and 4, respectively, while solid squares correspond to $\lambda=8$.

been carried out. The average self-diffusion coefficient is found to decrease with increasing concentration and dipolar interaction strength, but to be independent of the magnetic field strength. These results are in agreement with the predictions of a simplified mean-field model [6]. In the presence of a magnetic field, anisotropic self-diffusion is observed and the dependence of the parallel and perpendicular diffusion coefficients on the strength of the applied field, the particle concentration, and the dipolar interaction strength is studied. For moderate concentrations and interaction strengths, the diffusion coefficients are found to scale as $D_{\parallel,\perp} \propto L_2(h)$, where h is the Langevin parameter. Interestingly, we find $D_\parallel < D_\perp$, which corresponds to effective oblate particles. This finding is in agreement with mean-field predictions [24] on the rheological properties of the model ferrofluid in the weakly interacting regime. Our results in Fig. 9, as well as in previous computer simulation studies [25,26] on very similar model systems have shown that significant cluster formation starts only for higher dipolar interaction strengths $\lambda^* \gtrsim 8$. Thus, one might expect a crossover to a regime with $D_\parallel > D_\perp$ which is typical for the diffusion of chainlike aggregates at those interaction strengths. Diffusion coefficients for solutions of semiflexible chains have been discussed, e.g., in [27].

Experimental studies on dilute, weakly interacting ferrofluids would be extremely interesting in order to compare the results to those of the present study. On the other hand, further simulations should be carried out in order to investigate the effect of hydrodynamic interactions on the coefficients of self-diffusion. From these simulations also, the gradient-diffusion coefficients can be obtained. Research in that direction is currently under way.

ACKNOWLEDGMENTS

The authors are grateful to S. Hess for valuable discussions. Financial support by DFG-SPP 1104, "Kolloidale magnetische Fluide," Grant No. HE1104/03, is gratefully acknowledged. P.I. is supported by the Alexander von Humboldt Foundation. Most of the computations have been performed at the Linux Beowulf cluster, ETH Zürich.

[1] *Ferrofluids. Magnetically Controllable Fluids and Their Applications*, edited by S. Odenbach, Lecture Notes in Physics Vol. 594 (Springer, Berlin, 2002).
[2] J. Lal, D. Abernathy, L. Auvray, O. Diat, and G. Grübel, Eur. Phys. J. E **4**, 263 (2001).
[3] J.-C. Bacri, A. Cebers, A. Bourdon, G. Demouchy, B. M. Heegaard, and R. Perzynski, Phys. Rev. Lett. **74**, 5032 (1995).
[4] K. I. Morozov, J. Magn. Magn. Mater. **122**, 98 (1993).
[5] E. Blums, J. Magn. Magn. Mater. **149**, 111 (1995).
[6] P. Ilg, Phys. Rev. E **71**, 051407 (2005).
[7] M. Kollmann, R. Hund, B. Rinn, G. Nägele, K. Zahn, H. König, G. Maret, R. Klein, and J. K. G. Dhont, Europhys. Lett. **58**, 919 (2002).
[8] M. Hernández-Contreras, P. González-Mozuelos, O. Alarcón-Waess, and H. Ruíz-Estrada, Phys. Rev. E **57**, 1817 (1998).
[9] M. Hernández-Contreras and H. Ruíz-Estrada, Phys. Rev. E **68**, 031202 (2003).
[10] R. E. Rosensweig, *Ferrohydrodynamics* (Cambridge University Press, Cambridge, UK, 1985).
[11] P. Ilg, M. Kröger, and S. Hess, Phys. Rev. E **71**, 051201 (2005).
[12] H. C. Öttinger, *Stochastic Processes in Polymeric Fluids* (Springer, Berlin, 1996).
[13] J. A. Barker and D. Henderson, J. Chem. Phys. **47**, 4714 (1976).
[14] R. Gomer, Rep. Prog. Phys. **53**, 917 (1990).
[15] A. Leshansky and J. Brady, J. Fluid Mech. **527**, 141 (2005).
[16] E. J. Maginn, A. T. Bell, and D. N. Theodorou, J. Phys. Chem. **97**, 4173 (1993).
[17] R. DeHoff and N. Kulkarni, Mater. Res. **5**, 209 (2002).
[18] M. Marchioro and A. Acrivos, J. Fluid Mech. **443**, 101 (2001).
[19] M. P. Allen and D. J. Tildesley, *Computer Simulation of Liquids* (Oxford University Press, Oxford, UK, 1987).
[20] D. M. Heyes and A. C. Branka, Mol. Phys. **98**, 1949 (2000).
[21] A. Y. Zubarev and L. Y. Iskakova, JETP **80**, 857 (1995).
[22] A. Y. Zubarev, S. Odenbach, and J. Fleischer, J. Magn. Magn. Mater. **252**, 241 (2002).
[23] R. Vasanthi, S. Bhattacharyya, and B. Bagchi, J. Chem. Phys. **116**, 1092 (2002).
[24] P. Ilg and S. Hess, Z. Naturforsch., A: Phys. Sci. **58a**, 589 (2003).
[25] Z. Wang, C. Holm, and H. W. Müller, Phys. Rev. E **66**, 021405 (2002).
[26] H. Morimoto and T. Maekawa, J. Phys. A **33**, 247 (2000).
[27] M. Kröger, Phys. Rep. **390**, 453 (2004).